

The enigmatic 12/5 fractional quantum Hall effect

Kiryl Pakrouski¹, Matthias Troyer^{1,2,3}, Yang-Le Wu⁴, Sankar Das Sarma⁴ and Michael R. Peterson⁵

¹*Theoretische Physik and Station Q Zurich, ETH Zurich, 8093 Zurich, Switzerland*

²*Quantum Architectures and Computation Group, Microsoft Research, Redmond, WA, USA*

³*Microsoft Research Station Q, Santa Barbara, CA, USA*

⁴*Joint Quantum Institute and Condensed Matter Theory Center, Department of Physics, University of Maryland, College Park, Maryland 20742, USA and*

⁵*Department of Physics & Astronomy, California State University Long Beach, Long Beach, California 90840, USA*

(Dated: November 12, 2018)

We numerically study the fractional quantum Hall effect at filling factors $\nu = 12/5$ and $13/5$ (the particle-hole conjugate of $12/5$) in high-quality two-dimensional GaAs heterostructures via exact diagonalization including finite well width and Landau level mixing. We find that Landau-level mixing suppresses the $\nu = 13/5$ fractional quantum Hall effect relative to $\nu = 12/5$. By contrast, we find both $\nu = 2/5$ and (its particle-hole conjugate) $\nu = 3/5$ fractional quantum Hall effects in the lowest Landau level to be robust under Landau-level mixing and finite well-width corrections. Our results provide a possible explanation for the experimental absence of the $13/5$ fractional quantum Hall state as caused by Landau-level mixing effects.

PACS numbers: 71.10.Pm, 71.10.Ca, 73.43.-f

I. INTRODUCTION

There is interest across physics, mathematics, engineering, materials research, and computer science in finding robust experimental manifestations of topologically ordered phases with non-Abelian anyonic low-energy excitations. Not only are non-Abelian anyons (i.e., neither fermions nor bosons) suitable for topological quantum computation, but they are described by topological quantum field theories (TQFTs) of intrinsic fundamental interest¹. The fractional quantum Hall effect²⁻⁴ (FQHE) is the canonical example of a system supporting topologically ordered phases and is widely thought to support non-Abelian anyons in the second orbital electronic Landau level (LL), most probably at filling factor $\nu = 5/2$ ⁵. There is a possibility that the experimentally observed FQHE at $\nu = 12/5$ supports particularly exotic topologically ordered phases described by the Z_3 parafermionic Read-Rezayi states⁶⁻¹³, exemplifying an exotic $SU(2)_3$ TQFT [in contrast to the $5/2$ FQH state belonging to the $SU(2)_2$ TQFT]. Since $SU(2)_3$ TQFT supports a richer version of non-Abelian anyons that can realize *universal* fault-tolerant quantum computation¹, there is a great deal of interest in the $12/5$ FQHE. In this work, we focus on the enigmatic FQHE at $\nu = 12/5$.

Compared to the rather ubiquitous $\nu = 5/2$ FQHE, the experimental literature for $\nu = 12/5$ ($= 2 + 2/5$ filling) is sparse with only a few experimental reports of its observation. The $12/5$ FQHE was observed in a 30 nm wide GaAs quantum well with electron densities of $n \sim 3 \times 10^{11} \text{cm}^{-2}$ at magnetic field strengths of $B \sim 5$ Tesla at temperatures $T \sim 6\text{-}36$ mK¹⁴⁻¹⁹. In addition to its fragility (the $12/5$ FQHE is observed only in the highest quality samples with little disorder), the real enigma is the corresponding particle-hole conjugate FQHE at $13/5$ ($= 5 - 12/5$), which has never been observed in spite of other FQHEs in the second LL (e.g., $7/3$ and $8/3$, $11/5$ and $14/5$) showing both particle-hole conjugate states with roughly equal strength. This discrepancy is puzzling because in the lowest LL the FQHEs at $\nu = 2/5$ and $3/5$ are both routinely observed, are to good approximation particle-

hole conjugates of one another²⁰⁻²², and are well-described by the composite fermion (CF) theory^{4,23}. The exotic, rather than CF-like nature of the $12/5$ state has been discussed based on the analysis of the experimentally measured energy gap¹⁵. Interestingly, the $12/5$ and $13/5$ FQHEs (with roughly equal strength) are observed in systems where two subbands are occupied (e.g., bilayers, thick quantum wells) such that the chemical potential is in the lowest LL (but in the higher subband so two LLs are completely full)²⁴⁻²⁶. In this work we provide a possible explanation for the absence (presence) of a $13/5$ ($12/5$) FQHE in the second LL as arising from the LL mixing effect that explicitly breaks the particle-hole symmetry.

Several candidate wave functions for $\nu = 12/5$ have been proposed and studied⁸⁻¹⁰ under idealized conditions, using the Coulomb interaction without particle-hole symmetry breaking. Two recent numerical studies^{9,10} reinforced initial results^{6,7} that the ground state at $\nu = 12/5$ is in the non-Abelian Z_3 Read-Rezayi (RR) phase. Both studies perturbed the interaction finding a finite region of stability around the Coulomb point. All works considered particle-hole symmetric two-body Hamiltonians, so all conclusions made therein regarding the $\nu = 12/5$ state are equally valid for the particle-hole conjugate state at $\nu = 13/5$. Thus, existing theories provide evidence that the experimentally observed $12/5$ and (unobserved) $13/5$ FQHEs are both in the RR Z_3 phase, but cannot explain *why* one (i.e., $12/5$) exists experimentally and the other (i.e., $13/5$) does not. We provide a plausible explanation for this puzzle.

LL mixing breaks particle-hole symmetry through emergent three-body (and higher) terms in an effective realistic Hamiltonian²⁷⁻³⁰. The importance of LL mixing can be parameterized by the ratio κ of the Coulomb energy $e^2/\epsilon l_0$ to the bare cyclotron energy $\hbar\omega$ (i.e., the LL gap): $\kappa = (e^2/\epsilon l_0)/\hbar\omega$, where ϵ is the background lattice dielectric constant, $l_0 = \sqrt{\hbar c/eB}$ is the magnetic length, e is the electron charge, and $\omega = eB/mc$ is the cyclotron frequency. For GaAs, $\kappa \approx 2.5/\sqrt{B[\text{T}]}$. For most experiments in the second LL, κ is

of the order of unity, making LL mixing an important correction. One attempt at incorporating LL mixing at $\nu = 12/5$ used the approximation of including additional basis states within exact diagonalization³¹, but did not investigate 13/5.

In the present work, we numerically study a realistic model of the FQHE in the second LL using exact diagonalization, systematically including LL mixing effects due to (the infinite number of) all other LLs. We find that the LL mixing-induced particle-hole symmetry breaking strongly favors the $\nu = 12/5$ FQHE over the 13/5 in the second LL, qualitatively in agreement with experimental observations. By contrast, in the lowest LL, we do not find significant particle-hole symmetry breaking between $\nu = 2/5$ and 3/5 FQHE. Our work gives a probable explanation for the presence (absence) of 12/5 (13/5) in the second LL and the existence and equal strength of 2/5 and 3/5 FQHEs in the lowest LL. Our work also strengthens the claim that at finite LL mixing, a 12/5 FQHE arises from a RR parafermionic non-Abelian state (rather than from Abelian composite fermion states as for the 2/5 and 3/5 FQHEs).

II. EFFECTIVE HAMILTONIAN

Our realistic effective Hamiltonian describes N_e interacting electrons confined to the N^{th} LL of a quasi-two-dimensional quantum well (modeled as an infinitely deep square well of width w) and incorporates LL and subband mixing. The Coulomb interaction causes virtual electron/hole excitations to higher/lower LLs and subbands included perturbatively to lowest order in κ (note this involves coupling all LLs²⁸). The effective Hamiltonian is

$$H(w/\ell_0, \kappa, N) = \sum_m V_{2\text{body},m}^{(N)}(w/\ell_0, \kappa) \sum_{i<j} \hat{P}_{ij}(m) + \sum_m V_{3\text{body},m}^{(N)}(w/\ell_0, \kappa) \sum_{i<j<k} \hat{P}_{ijk}(m) \quad (1)$$

where $\hat{P}_{ij}(m)$ and $\hat{P}_{ijk}(m)$ are two- and three-body projection operators onto pairs or triplets of electrons with relative angular momentum m . $V_{2\text{body},m}^{(N)}(w/\ell_0, \kappa)$ and $V_{3\text{body},m}^{(N)}(w/\ell_0, \kappa)$ are the two- and three-body effective pseudopotentials^{32,33} in the N^{th} LL. The full calculation of the two- and three-body pseudopotentials is quite involved and is given in detail in Ref. 28 for systems with finite thickness, in Ref. 29 for zero thickness, and in Ref. 30 where the calculation is done numerically. Here we provide a brief outline of the main details and encourage the reader to consult the above references.

In the absence of Landau level (LL) mixing, the planar pseudopotentials $V_{2\text{body},m}^{(N)}$ can be calculated as (see, for instance, Ref. 4)

$$V_{2\text{body},m}^{(N)} = \int_0^\infty q dq V(q) [L_N(q^2/2)]^2 L_m(q^2) e^{-q^2}, \quad (2)$$

where N is the LL index, L_N are the Laguerre polynomials,

and

$$V(q) = \frac{1}{2\pi} \int d^2\mathbf{r} e^{i\mathbf{q}\cdot\mathbf{r}} V(r) \quad (3)$$

is the Fourier transform of the real-space interaction potential $V(r)$. For the case of finite width, $V(q)$ can be written as

$$V(q) = \frac{e^2}{\epsilon q} \int dz_1 \int dz_2 |\eta(z_1)|^2 |\eta(z_2)|^2 e^{-q|z_1 - z_2|}, \quad (4)$$

where $\eta(z)$ is the electron wave function in the z -direction. For a realistic experimental system, $\eta(z)$ can be determined from solving the Schrodinger and Poisson equations self-consistently (see Ref. 4 for more details). In this work, we consider an infinitely deep square well of width w to model finite thickness, hence, $\eta(z) = \sqrt{2/w} \sin(\pi z/w)$.

Pseudopotentials describing the pure Coulomb interaction can be derived in both the spherical and planar geometries. Because the planar pseudopotentials do not depend on the system size it is more convenient to compute the pseudopotentials that include effects of finite thickness and Landau-level mixing in the planar geometry. The spherical pseudopotentials extrapolate to the planar pseudopotentials in the limit of a sphere of infinite radius, i.e., the thermodynamic limit. Further, it has been demonstrated that using planar pseudopotentials in the spherical geometry does not lead to qualitative differences compared with using spherical pseudopotentials (see for example Ref. 34).

Beyond renormalizing the two-body interactions, LL mixing produces particle-hole symmetry breaking three-body terms (cf. Ref. 28). Equation (1) has a well-defined exact limit as $\kappa \rightarrow 0$, hence, we can determine the leading-order effects of LL mixing on the FQHE. Most experimental observations of the 12/5 FQHE occur at fields of $B \sim 5.15$ T (see Ref. 15), giving a quantum well width (30 nm) of $w/l_0 \approx 2.65$ and $\kappa \approx 1.1$. We estimate (an exact self-consistent calculation is possible for a particular device³⁴) that an infinitely deep quantum well of $w/l_0 \approx 3$ provides approximately the same confinement as the real quantum well, and we consider $w/l_0 \leq 4$ and $\kappa \neq 0$ to model realistic samples under realistic conditions. We assume fully spin-polarized¹⁰ single-component states throughout this work. We consider $V_{3\text{body},m}^{(1)}$ for $3 \leq m \leq 8$ —previous work demonstrated that $m > 9$ terms are unlikely to produce qualitative effects³⁴, especially for small κ .

We use the spherical geometry^{4,32} with the total magnetic flux $N_\phi = N_e/f - S$, and where f is the filling factor, as $N_e \rightarrow \infty$, of the N^{th} LL and S is the shift³⁵. The experimental filling factor is $\nu = f + 2N$, where $2N$ arises from completely filling the lower N spin-up and -down LLs. FQHE states are gapped uniform density ground states with total angular momentum $L = 0$. The RR Z_3 state describes $f = 3/5$ with $S = 3$, while the particle-hole conjugate RR state, $\text{conj}(Z_3)$, describes $f = 2/5$ with $S = -2$. The CF states for $\nu = 2/5$ and 3/5 have shifts of $S = 4$ and -1 , respectively. Although the pairs of particle-hole conjugate states appear at different shifts, in the absence of LL mixing ($\kappa = 0$) they have identical spectra and all eigenstates are particle-hole

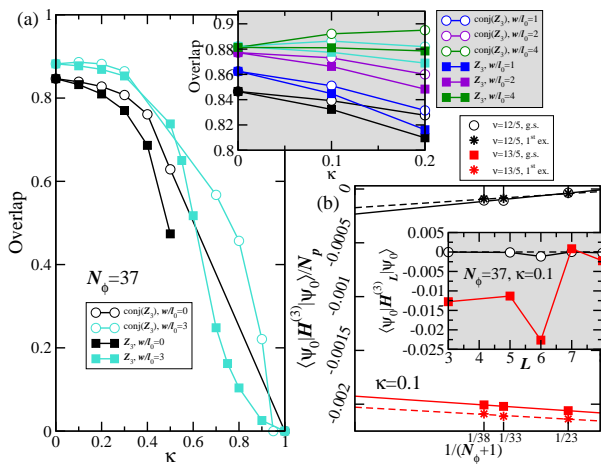


FIG. 1. (Color online) (a) Wave-function overlap between Z_3 and $\text{conj}(Z_3)$ and the exact ground state of Eq. (1) at $\nu = 13/5$ and $12/5$, respectively, as a function of κ for $N_\phi = 37$ (14 holes/electrons). A finite well width increases the overlaps and κ breaks particle-hole symmetry, yielding higher overlaps with $\text{conj}(Z_3)$ for $12/5$ compared to Z_3 for $13/5$. The inset shows the overlaps in more detail. (b) Expectation values of the three-body terms per particle N_p of Eq. (1) for $\kappa = 0.1$ and $w/l_0 = 0$, evaluated for the ideal Coulomb ground and first excited states (both denoted $|\psi_0\rangle$) at $12/5$ and $13/5$, respectively, as a function of inverse LL degeneracy $[1/(N_\phi + 1)]$ extrapolated to the thermodynamic limit. $N_\phi = 27$ is aliased with $\nu = 1/3$ and left out. Inset: Expectation values for each three-body term $[H_L^{(3)} = V_{3\text{body},L}^{(N)}(w/l_0, \kappa = 0.1) \sum_{i < j < k} \hat{P}_{ijk}(L)]$ for $N_\phi = 37$. Lines are a guide to the eye, except in the main plot of (b) where they represent linear extrapolations.

conjugates of each other. Hence, by considering properties such as energy gaps, overlaps, and entanglement spectra, we can isolate the effects of LL mixing.

III. OVERLAP, PERTURBATION THEORY, AND ENTANGLEMENT SPECTRA

We first investigate whether the system remains in the Z_3 RR phase under realistic conditions. The ground state of Eq. (1) is uniform with $L = 0$ for the RR shifts for all system sizes up to $N_\phi = 37$ for $\kappa \neq 0$ and $N_\phi = 42$ for $\kappa = 0$ (we have not studied $\kappa \neq 0$ for $N_\phi = 42$). The ground states have $L \neq 0$ for the CF shifts for zero and non-zero κ , for most system sizes. The Bonderson-Slingerland (BS) non-Abelian state for $\nu = 12/5$ ³⁷ has $L = 0$ at $\kappa = 0$, but a smaller gap than the RR state⁸—this behavior remains with $\kappa \neq 0$; see Appendix A. Similar qualitative results were recently found in the $\kappa = 0$ limit^{9,10}.

Figure 1(a) presents the overlap between the exact ground state $|\psi\rangle$ of Eq. (1) with the model wave functions [Z_3 and $\text{conj}(Z_3)$]. For small κ , the overlap remains relatively unchanged, but the $12/5$ overlap with $\text{conj}(Z_3)$ is larger than the overlap with Z_3 at $13/5$ for $\kappa \lesssim 0.5$ for all system sizes—the overlap at $13/5$ decreases monotonically with κ and both overlaps are found to collapse to zero near $\kappa \approx 1$, though some

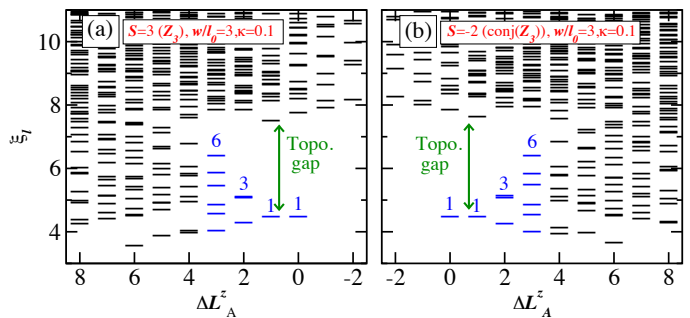


FIG. 2. (Color online) Entanglement spectrum for the exact ground state of Eq. (1) for $w/l_0 = 3$ and $\kappa = 0.1$ at (a) $\nu = 13/5$ (shift $S = 3$) and (b) $\nu = 12/5$ (shift $S = -2$) for $N_\phi = 37$. The counting for the low-lying levels is 1, 1, 3, and 6 up to $\Delta L_A^z = 5$, agreeing with Z_3 and $\text{conj}(Z_3)$. The orbital cuts, using the notation of Ref. 36, are $P[0|0]$ for $S = 3$ and $P[1|1]$ for $S = -2$. $\Delta L_A^z = L_A^z - (L_A^z)_{\text{root}}$ where (a) $(L_A^z)_{\text{root}} = 120$ and (b) $(L_A^z)_{\text{root}} = 60.5$. The topological gap is indicated by the green arrow and defined as the difference between the two lowest-lying levels at $\Delta L_A^z = 1$ (see Sec. IV).

finite-size effects are observed for larger κ .

Since the overlaps are relatively flat for small κ , we study the eigenstates obtained in the absence of LL mixing, at $\kappa = 0$ (denoted $|\psi_0\rangle$). We calculate $\langle \psi_0 | H^{(3)}(\kappa = 0.1) | \psi_0 \rangle$, where $H^{(3)}(\kappa) = \sum_m V_{3\text{body},m}^{(N)}(w/l_0, \kappa) \sum_{i < j < k} \hat{P}_{ijk}(m)$ [shown in Fig. 1(b)]—this represents the lowest-order perturbative contribution to particle-hole symmetry breaking induced by LL mixing. The thermodynamic limit extrapolation of $\langle \psi_0 | H^{(3)}(\kappa = 0.1) | \psi_0 \rangle$ per particle for $\nu = 12/5$ is more than ten times smaller than for $13/5$, indicating that LL mixing more severely affects the energetics of $13/5$ compared to $12/5$. While the ground-state energies are lowered by the three-body terms, the excited states are lowered as well, reducing the energy gap at $13/5$ and increasing the gap at $12/5$. In the inset of Fig. 1(b), we show that $V_{3\text{body},3}^{(1)}$, $V_{3\text{body},5}^{(1)}$, and $V_{3\text{body},6}^{(1)}$ are the three-body pseudopotentials that contribute most to particle-hole symmetry breaking between $\nu = 12/5$ and $13/5$. The Z_3 state has a relative abundance of three-body clustering by construction⁶ and large expectation value of $H^{(3)}(\kappa)$ (not shown), similar to $|\psi_0\rangle$ at $\nu = 13/5$. In contrast, the three-body terms have little effect on $12/5$.

Overlaps may depend on short-range physics, so we investigate orbital entanglement spectra^{36,38–42}. If the ground state is in the RR phase, the counting of the low-lying levels of the entanglement spectra will be related to the $SU(2)_3$ TQFT describing the edge excitations³⁶. The counting of the low-lying levels for $\nu = 13/5$ and $12/5$ for $w/l_0 = 3$ and $\kappa = 0.1$ (Fig. 2) matches the counting for Z_3 and $\text{conj}(Z_3)$, respectively, (including $\kappa = 0$; see Ref. 9).

The results above confirm that the ground state of Eq. (1) remains in the RR phase under LL mixing. Further, LL mixing affects $\nu = 13/5$ more than $12/5$ and introduces strong particle-hole asymmetry.

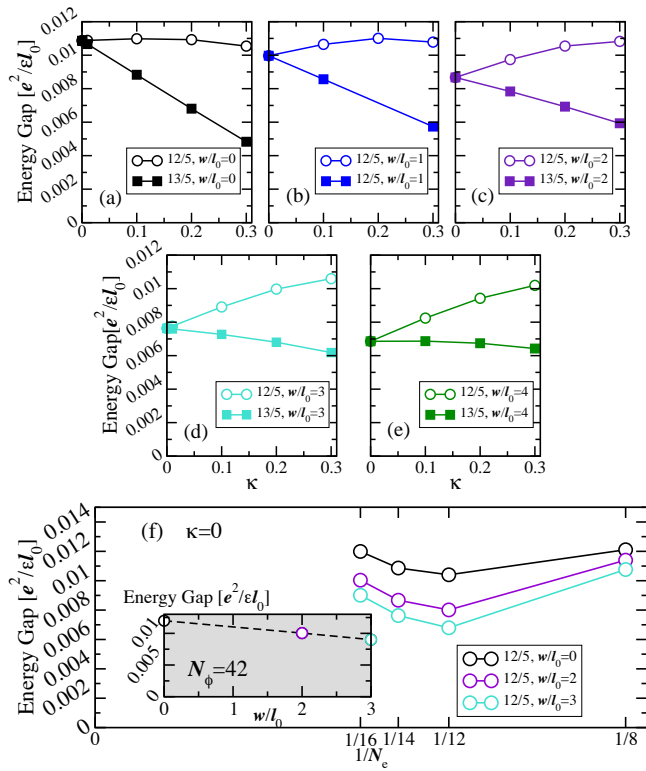


FIG. 3. (Color online) Energy gap for $N_\phi=37$ at $\nu = 12/5$ and $13/5$ for (a)-(e) $w/l_0 = 0-4$. Similar results are obtained for smaller system sizes. (f) Width dependence of the gap for $N_e = 8, 12, 14$, and 16 for $\nu = 12/5$ for $w/l_0 = 0, 2$, and 3 and $\kappa = 0$. Inset: The gap as a function of w/l_0 at $\kappa = 0$ for $N_e = 16$ ($N_\phi = 42$). Finite width reduces the gap by approximately 25% at $w/l_0 = 3$ relative to $w/l_0 = 0$ for the largest system size. Note the similarities in (f) to Fig. 1(b) in Ref. 9.

IV. ENERGY GAP AND TOPOLOGICAL GAP

The neutral gap is related to the experimentally measured activation gap and the physical robustness of the FQHE. It is the difference between the two lowest energies at constant N_ϕ , if the ground state has $L = 0$, otherwise it is taken to be zero.

Figure 3(a)-3(e) show energy gaps for our largest system ($N_\phi = 37$) for $w/l_0 = 0-4$, respectively. LL mixing breaks particle-hole symmetry, producing a larger energy gap for $\nu = 12/5$ compared to $13/5$. The gap at $w/l_0 \neq 0$ for $12/5$ increases with κ , while the $13/5$ gap is suppressed (the suppression is found for all non-aliased system sizes and values of w/l_0); however, an increasing gap at $\nu = 12/5$ for non-zero width is only found for the two largest system sizes $N_\phi = 37$ and 32 . Hence, LL mixing strengthens the $12/5$ FQHE for finite w/l_0 , while weakening $13/5$ (strengthening of the FQHE gap with LL mixing does not happen for $\nu = 5/2^{34}$).

The thermodynamic extrapolation suffers from finite-size effects ($N_\phi = 12$ and 17) and aliasing ($N_\phi = 27$). The energy gaps at the remaining N_ϕ are shown in Fig. 3(f). Without LL mixing, finite width decreases the gap from $0.012e^2/\epsilon l_0$ at $w/l_0 = 0$ to $0.009e^2/\epsilon l_0$ at $w/l_0 = 3$ [values given are for

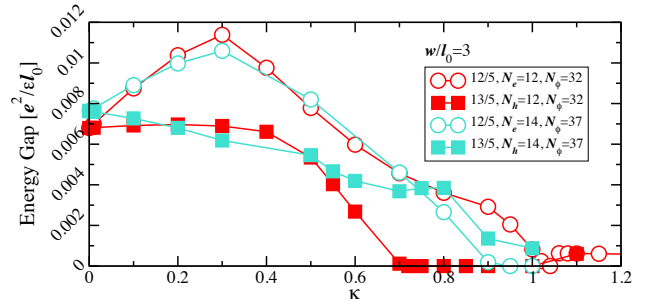


FIG. 4. (Color online) Energy gap for $\nu = 12/5$ and $13/5$ as a function of κ for $w/l_0 = 3$ for $N_\phi = 32$ and 37 . Energy gap for 12 holes at $13/5$ is put to 0 for $\kappa \geq 0.72$, where the ground state has gone through a phase transition into a non-homogeneous state with $L = 2$. We note for $\kappa \gtrsim 0.6$ the gap behavior is no longer consistent between system sizes.

$N_\phi = 42$, shown in the inset of Fig. 3(f)). In the limit of small LL mixing, (i.e., high magnetic fields), it should be possible to observe more robust $12/5$ states in narrow quantum wells.

We expect that the equivalence of various models of finite width demonstrated for $\nu = 5/2^{34}$ also holds here. Thus, to determine the effective width w/l_0 corresponding to a certain experimental device, one would first calculate (for instance, using a Schrodinger-Poisson solver) or measure⁴³ the square of the absolute value of the electron wave function in the direction perpendicular to the two-dimensional electron gas (2DEG) and determine its variance (as defined in Ref. 34). Then, w/l_0 should be chosen such that the variance in the ground state of an infinitely deep quantum well of width w/l_0 is the same as in the given experimental sample.

Figure 4 shows the energy gap as a function of κ for $N_\phi = 32$ and 37 [12 and 14 electrons (holes) for $\nu = 12/5$ ($13/5$), respectively] to the experimental value of $\kappa \sim 1.1$ for $w/l_0 = 3$. All of the sharp features in the κ -dependence are associated with the change of L in the first-excited states. The behavior of the different system sizes is consistent up to $\kappa = 0.6 - 0.7$ and demonstrates a larger energy gap at $12/5$ than at $13/5$. Finite-size effects are observed for larger κ , which could be a result of our perturbative (in κ) approach to LL mixing breaking down or the smallness of the energy gap.

Finally, we investigate the topological gap. Following Ref. 36, we define the topological gap as the difference between the two lowest-lying levels in the entanglement spectrum at $\Delta L_A^z = 1$ (see Fig. 2). It represents the “energy difference” between the universal part of the entanglement spectrum, describing the [non-Abelian in the case of RR and conj(RR)] modes and the generic continuum of states. In Fig. 5, we identify two trends: first, the topological gap increases with increased finite width, and second, Landau-level mixing leads to the suppression of the topological gap at $13/5$ relative to $12/5$ in the same way as observed for the energy gap, giving support to the main conclusion of this work based on a different measure.

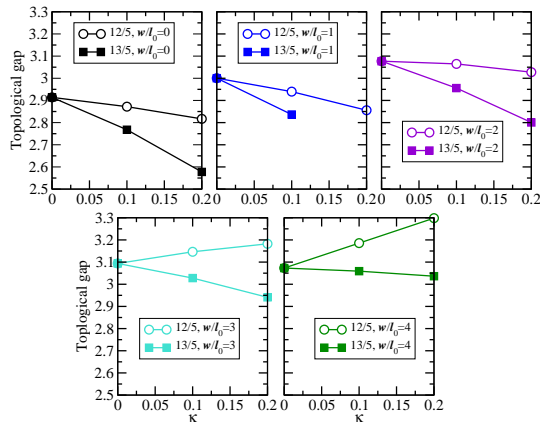


FIG. 5. (Color online) Topological gap for 12/5 and 13/5 as a function of κ for $w/l_0 = 0-4$ and $N_\phi = 37$.

V. SECOND VERSUS LOWEST LANDAU LEVEL

Finally, we compare the second with the lowest LL. In Fig. 6(a), we show the relative energy gap difference induced by LL mixing between $\nu = 12/5$ and $13/5$ and between $\nu = 2/5$ and $3/5$ as a function of particle number. The LL mixing induced difference is much larger in the second LL than in the lowest LL (the sign is also different between the two, with 12/5 strongly favored in the second LL while 3/5 is slightly favored in the lowest LL). The LL mixing induced gap difference between 12/5 and 13/5 grows with system size and is likely a robust feature in the thermodynamic limit.

We can further quantify the particle-hole symmetry breaking by calculating the overlap between the exact ground state $|\psi\rangle$ at $\nu = 12/5$ (2/5) and the particle-hole conjugate of the exact ground state $|\text{conj}(\psi)\rangle$ at $\nu = 13/5$ (3/5). At $\kappa = 0$, this overlap is unity since the two states are particle-hole conjugates. In Fig. 6(b), particle-hole symmetry is much more strongly broken for the $\nu = 12/5$ (13/5) FQHE than for the $\nu = 2/5$ (3/5) FQHE. In fact, particle-hole symmetry is hardly broken at all in the lowest LL [in the lowest LL, $\langle\psi|\text{conj}(\psi)\rangle \gtrsim 0.9$ up to $\kappa \sim 2.4$]. This apparent particle-hole symmetry could be a property of the lowest LL or of the CF-like states in any LL.

VI. CONCLUSION

LL mixing strongly breaks the particle-hole symmetry between $\nu = 12/5$ and $13/5$ FQHE in the second LL, but has little effect on $\nu = 2/5$ and $3/5$ FQHE in the lowest LL. Our work implies that the absence of 13/5 FQHE in the second LL is likely a direct consequence of LL mixing effects. This is mainly due to the suppression of the energy gap at $\nu = 13/5$ – the FQHE might simply be too fragile (in terms of energy gap) since LL mixing affects 13/5 more severely than 12/5, and because in experimental measurements, at constant density, κ is larger at 13/5 compared to 12/5 (since the magnetic field at 13/5 is smaller than at 12/5). The 12/5 ground state

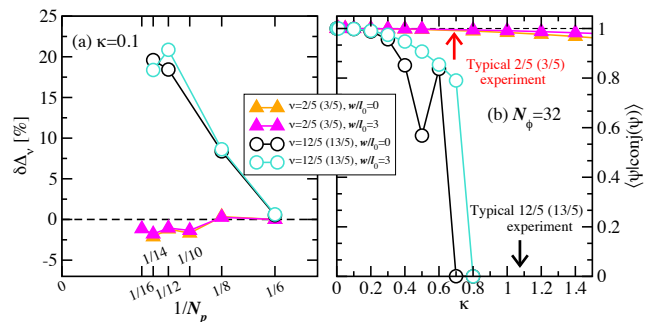


FIG. 6. (Color online) (a) Relative gap difference $\delta\Delta_\nu = (\Delta_\nu - \Delta_{1-\nu})/\Delta_\nu$ (induced by $\kappa = 0.1$) between particle-hole-conjugates at 12/5 (13/5) and 2/5 (3/5). N_p is the number of particles for $\nu = 12/5$ and 2/5 or number of holes for $\nu = 13/5$ and 3/5. (b) Particle-hole symmetry breaking [quantified by $\langle\psi|\text{conj}(\psi)\rangle$] in the second LL compared to the lowest LL for $w/l_0 = 0$ and 3. The system sizes are $N_\phi = 32$ for $\nu = 12/5$ (13/5) and $N_\phi = 31$ for $\nu = 2/5$ (3/5).

at shift $S = -2$ remains in the non-Abelian parafermionic (conjugate) RR Z_3 phase when finite-width and non-zero LL mixing are taken into account extending the validity of previous conclusions^{6,7,9,10,31} obtained for idealized conditions. We do not rule out the $\nu = 13/5$ FQHE in the Z_3 RR phase, but establish that the 13/5 FQHE is always much weaker than 12/5. Future experiments with smaller κ could show a very weak FQHE at $\nu = 13/5$ in extremely high-mobility samples at ultra-low temperatures with a very small activation energy.

ACKNOWLEDGMENTS

M.T. and K.P. were supported by the Schweizerischer Nationalfonds zur Förderung der Wissenschaftlichen Forschung, National Centre of Competence in Research – Quantum Science and Technology, the European Research Council, ERC Advanced Grant SIMCOFE and by Microsoft Research. M.R.P. was supported by the National Science Foundation under Grant No. DMR-1508290, the Office of Research and Sponsored Programs at California State University Long Beach, and the W. M. Keck Foundation. Y.L.W. and S.D.S. were supported by Microsoft Research and LPS-MPO-CMTC. This work was supported by a grant from the Swiss National Supercomputing Centre (SCSC) under Project IDs s395 and s551. The authors are grateful to C. Nayak, R. Mong, R. Morf, M. Zaletel, and also P. Bonderson and S. Simon for many helpful discussions.

Appendix A: Energetics at the Bonderson-Slingerland shift

In this appendix, we explore the perturbative change in the FQHE gap Landau-level mixing induced at the shifts corresponding to the Bonderson-Slingerland (BS) state and its corresponding particle-hole conjugate. Shown in Fig. 7 are the expectation values of the three-body terms of our effective Hamiltonian [Eq. (1)] for the ground and first-excited states

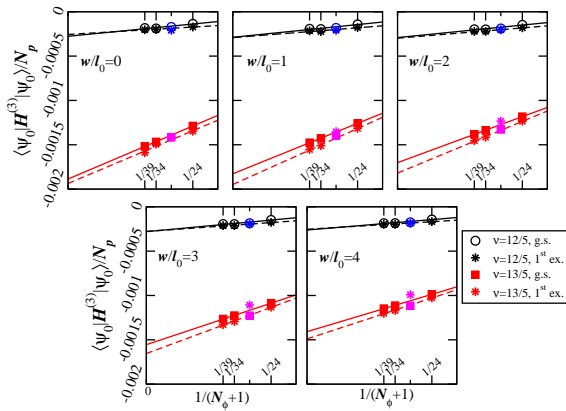


FIG. 7. (Color online) Expectation values of the three-body terms per particle N_p of Eq. (1) for $\kappa = 0.1$ and $w/l_0 = 0, 1, 2, 3,$ and 4 evaluated for the ideal Coulomb ground and first-excited states at $12/5$ and $13/5$, respectively, as a function of inverse Landau level degeneracy $[1/(N_\phi + 1)]$ extrapolated to the thermodynamic limit. The only difference from Fig. 1(b) is that the ground state at the Bonderson-Slingerland shift and its particle-hole conjugate ($S = 2$ and $S = 1/3$) were taken instead of the ones for the Read-Rezayi and conjugate shifts. Lines represent linear extrapolations, excluding the $N_\phi = 28$ data point which appears to behave differently from all other system sizes [these points are indicated in blue ($12/5$) and magenta ($13/5$), respectively.]

[the results are presented in the same way as in Fig. 1(b)]. Both the ground and excited states reduce their energy by approximately the same amount at $12/5$. For $13/5$, the energy of the excited state is reduced significantly more than that of the ground state meaning that the gap of $13/5$ is reduced, whereas the gap of $12/5$ remains relatively constant.

Appendix B: Robustness of the composite fermion states for the $2/5$ and $3/5$ FQHE under Landau level mixing

To further characterize the evolution of the states in the lowest Landau level, we approximate the CF-like states at $2/5$ and $3/5$ with the exact ground state of a “hard-core” model Hamiltonian with $V_1 \neq 0$ and all other $V_m = 0$ at $N_\phi = 5N_e/2 - 4$ and $N_\phi = 5N_e/3 + 1$, respectively. This Hamiltonian produces the $1/m$ Laughlin state exactly as the zero-energy ground state for $N_\phi = m(N_e - 1)$ and produces ground states with large overlaps (> 0.99) with CF wave functions for filling factor $\nu = n/(2pn + 1)$ at the appropriate flux as checked via Monte Carlo. As shown in Fig. 8, the overlap remains stable under Landau-level mixing and only starts to significantly decrease around $\kappa = 3 - 4$, well beyond the typical experimental values.

It is an open question whether the observed robustness of the FQH states at $2/5$ and $3/5$ is due to their CF-like nature or to the specific form of the effective interaction in the lowest Landau level.

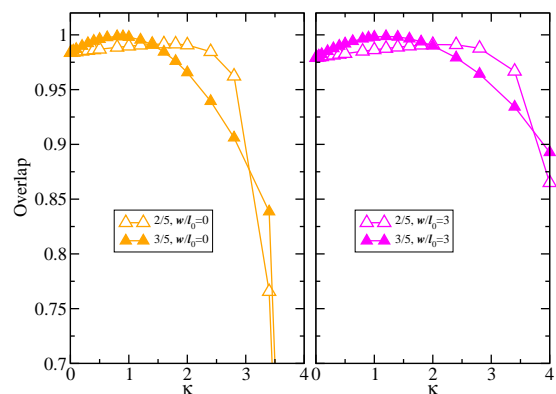


FIG. 8. (Color online) Overlap between the realistic ground state and the ground state of the hardcore ($V_1 \neq 0$ and $V_m = 0$ for all other m) Hamiltonian for $N_\phi = 31$. $w=0$ (left panel) and $w=3$ (right panel).

- ¹ C. Nayak, S. H. Simon, A. Stern, M. Freedman, and S. Das Sarma, *Rev. Mod. Phys.* **80**, 1083 (2008).
- ² D. C. Tsui, H. L. Stormer, and A. C. Gossard, *Phys. Rev. Lett.* **48**, 1559 (1982).
- ³ S. Das Sarma and A. Pinczuk, eds., *Perspectives in Quantum Hall Effects: Novel Quantum Liquids in Low-dimensional Semiconductor Structures* (Wiley, New York, 1997).
- ⁴ J. Jain, *Composite Fermions* (Cambridge University Press, 2007).
- ⁵ R. Willett, J. P. Eisenstein, H. L. Stormer, D. C. Tsui, A. C. Gossard, and J. H. English, *Phys. Rev. Lett.* **59**, 1776 (1987).
- ⁶ N. Read and E. Rezayi, *Phys. Rev. B* **59**, 8084 (1999).
- ⁷ E. H. Rezayi and N. Read, *Phys. Rev. B* **79**, 075306 (2009).
- ⁸ P. Bonderson, A. E. Feiguin, G. Möller, and J. K. Slingerland, *Phys. Rev. Lett.* **108**, 036806 (2012).
- ⁹ W. Zhu, S. S. Gong, F. D. M. Haldane, and D. N. Sheng, *Phys. Rev. Lett.* **115**, 126805 (2015).
- ¹⁰ R. S. K. Mong, M. P. Zaletel, F. Pollmann, and Z. Papić, ArXiv e-prints (2015), [arXiv:1505.02843 \[cond-mat.str-el\]](https://arxiv.org/abs/1505.02843).
- ¹¹ S. Geraedts, M. P. Zaletel, Z. Papić, and R. S. K. Mong, *Phys. Rev. B* **91**, 205139 (2015).
- ¹² M. R. Peterson, Y.-L. Wu, M. Cheng, M. Barkeshli, Z. Wang, and S. Das Sarma, *Phys. Rev. B* **92**, 035103 (2015).
- ¹³ Z. Liu, A. Vaezi, K. Lee, and E.-A. Kim, *Phys. Rev. B* **92**, 081102 (2015).
- ¹⁴ J. S. Xia, W. Pan, C. L. Vicente, E. D. Adams, N. S. Sullivan, H. L. Stormer, D. C. Tsui, L. N. Pfeiffer, K. W. Baldwin, and K. W. West, *Phys. Rev. Lett.* **93**, 176809 (2004).
- ¹⁵ A. Kumar, G. A. Csáthy, M. J. Manfra, L. N. Pfeiffer, and K. W.

West, *Phys. Rev. Lett.* **105**, 246808 (2010).

- ¹⁶ H. C. Choi, W. Kang, S. Das Sarma, L. N. Pfeiffer, and K. W. West, *Phys. Rev. B* **77**, 081301 (2008).

- ¹⁷ W. Pan, J. S. Xia, H. L. Stormer, D. C. Tsui, C. Vicente, E. D. Adams, N. S. Sullivan, L. N. Pfeiffer, K. W. Baldwin, and K. W. West, *Phys. Rev. B* **77**, 075307 (2008).

- ¹⁸ C. Zhang, C. Huan, J. S. Xia, N. S. Sullivan, W. Pan, K. W. Baldwin, K. W. West, L. N. Pfeiffer, and D. C. Tsui, *Phys. Rev. B* **85**, 241302 (2012).
- ¹⁹ N. Deng, J. D. Watson, L. P. Rokhinson, M. J. Manfra, and G. A. Csáthy, *Phys. Rev. B* **86**, 201301 (2012).
- ²⁰ R. R. Du, H. L. Stormer, D. C. Tsui, L. N. Pfeiffer, and K. W. West, *Phys. Rev. Lett.* **70**, 2944 (1993).
- ²¹ H. C. Manoharan, M. Shayegan, and S. J. Klepper, *Phys. Rev. Lett.* **73**, 3270 (1994).
- ²² W. Pan, (private communication).
- ²³ J. K. Jain, *Phys. Rev. Lett.* **63**, 199 (1989).
- ²⁴ Y. Liu, D. Kamburov, M. Shayegan, L. N. Pfeiffer, K. W. West, and K. W. Baldwin, *Phys. Rev. Lett.* **107**, 176805 (2011).
- ²⁵ Y. Liu, S. Hasdemir, J. Shabani, M. Shayegan, L. N. Pfeiffer, K. W. West, and K. W. Baldwin, *Phys. Rev. B* **92**, 201101 (2015).
- ²⁶ J. Shabani, Y. Liu, and M. Shayegan, *Phys. Rev. Lett.* **105**, 246805 (2010).
- ²⁷ W. Bishara and C. Nayak, *Phys. Rev. B* **80**, 121302 (2009).
- ²⁸ M. R. Peterson and C. Nayak, *Phys. Rev. B* **87**, 245129 (2013).
- ²⁹ I. Sodemann and A. H. MacDonald, *Phys. Rev. B* **87**, 245425 (2013).
- ³⁰ S. H. Simon and E. H. Rezayi, *Phys. Rev. B* **87**, 155426 (2013).
- ³¹ A. Wójs, *Phys. Rev. B* **80**, 041104 (2009).
- ³² F. D. M. Haldane, *Phys. Rev. Lett.* **51**, 605 (1983).
- ³³ S. H. Simon, E. H. Rezayi, and N. R. Cooper, *Phys. Rev. B* **75**, 195306 (2007).
- ³⁴ K. Pakrouski, M. R. Peterson, T. Jolicoeur, V. W. Scarola, C. Nayak, and M. Troyer, *Phys. Rev. X* **5**, 021004 (2015).
- ³⁵ X. G. Wen and Q. Niu, *Phys. Rev. B* **41**, 9377 (1990).
- ³⁶ H. Li and F. D. M. Haldane, *Phys. Rev. Lett.* **101**, 010504 (2008).
- ³⁷ P. Bonderson and J. K. Slingerland, *Phys. Rev. B* **78**, 125323 (2008).
- ³⁸ M. Levin and X.-G. Wen, *Phys. Rev. Lett.* **96**, 110405 (2006).
- ³⁹ A. Kitaev and J. Preskill, *Phys. Rev. Lett.* **96**, 110404 (2006).
- ⁴⁰ M. Haque, O. Zozulya, and K. Schoutens, *Phys. Rev. Lett.* **98**, 060401 (2007).
- ⁴¹ O. S. Zozulya, M. Haque, K. Schoutens, and E. H. Rezayi, *Phys. Rev. B* **76**, 125310 (2007).
- ⁴² J. Biddle, M. R. Peterson, and S. Das Sarma, *Phys. Rev. B* **84**, 125141 (2011).
- ⁴³ C. Reichl, W. Dietsche, T. Tschirky, T. Hyart, and W. Wegscheider, *New Journal of Physics* **17**, 113048 (2015).